A&A, 709, A255 (2026)
https://doi.org/10.1051/0004-6361/202659618

Astronomy & Astrophysics

Formation of benzene and its derivatives in dense molecular clouds

Jean-Christophe Loison[1,⋆], Ugo Jacovella[2,⋆], Corentin Rossi[2], Anne P. Rasmussen[2,3], Roland Thissen[4,5], Nandana Pattathadathil[4,6], Christian Alcaraz[4], and Valentine Wakelam[7]

[1] Université Bordeaux, CNRS, Bordeaux INP, ISM, UMR 5255, 33400 Talence, France
[2] Université Paris-Saclay, CNRS, Institut des Sciences Moléculaires d'Orsay, 91405 Orsay, France
[3] Department of Physics and Astronomy, Aarhus University, Ny Munkegade 120, 8000 Aarhus C, Denmark
[4] Université Paris-Saclay, CNRS, Institut de Chimie Physique, UMR8000, 91405 Orsay, France
[5] Synchrotron SOLEIL, L'Orme des Merisiers, 91192 Saint Aubin, Gif-sur-Yvette, France
[6] Department of Physics, University of Trento, Via Sommarive 14, 38123 Trento, Italy
[7] Laboratoire d'astrophysique de Bordeaux, Univ. Bordeaux, CNRS, B18N, allée Geoffroy Saint-Hilaire, 33615 Pessac, France

Received 26 February 2026 / Accepted 7 April 2026

ABSTRACT

Context. A number of aromatic molecules and small polycyclic aromatic hydrocarbons have recently been detected in dense molecular clouds, notably in TMC-1. Although these species are generally assumed to form through bottom-up chemical processes, current astrochemical models underestimate their abundances by several orders of magnitude.
Aims. This work aims to identify and constrain the dominant chemical pathways leading to the formation of the first six-carbon aromatic compounds in dense molecular clouds.
Methods. We revisited the chemistry of aromatic compounds in dense molecular clouds by systematically examining all neutral and ionic reactions that may lead to the formation of C_6H_6 and chemically related species (C_6H_4, C_6H_5, $C_6H_5^+$, $C_6H_6^+$, and $C_6H_7^+$). Each reaction was analyzed according to its relevance to the formation of the first aromatic compounds.
Results. We identified a limited number of key reactions that dominate the formation of the first aromatic ring. We found that ionic pathways involving l-$C_3H_3^+$ and l-$C_3H_5^+$ reacting with C_3H_4, together with the neutral reaction C + c-C_5H_6, are the main contributors to benzene formation. With the revised chemical network, the observed abundances of C_6H_4, C_6H_5CN, and $C_6H_5C_2H$ in TMC-1 can be reproduced within a factor of 2. This result is notably better than what has been achieved with previous models.
Conclusions. The revised bottom-up chemical scheme successfully reproduces the observed abundances of C_6 aromatic compounds, with significant uncertainties due to the lack of precise determinations for the branching ratios for many of the reactions involved. It also demonstrates the central role of neutral and ionic C_3 chemistry. The formation pathways of larger aromatic compounds remain to be explored.

Key words. astrochemistry – ISM: molecules – ISM: individual objects: TMC-1

1. Introduction

The first unambiguous detections of aromatic molecules and polycyclic aromatic hydrocarbons (PAHs) in the interstellar medium were recently reported, mainly toward the dark cloud Taurus Molecular Cloud 1 (TMC-1). These include cyclopentadiene (C_5H_6) and indene (C_9H_8; Cernicharo et al. 2021a; Burkhardt et al. 2021), ethynylbenzene ($C_6H_5C_2H$; Loru et al. 2023), o-benzyne (o−C_6H_4; Cernicharo et al. 2021b), fulvenallene ($C_5H_4CCH_2$; Cernicharo et al. 2022), and phenalene ($C_{13}H_{10}$; Cernicharo et al. 2021b). In addition, several cyano derivatives have been identified, including benzonitrile (C_6H_5CN; McGuire et al. 2018), cyanocyclopentadiene (C_5H_5CN; McCarthy et al. 2021), cyanonaphthalene ($C_{10}H_7CN$; McGuire et al. 2021), cyanoindene (C_9H_7CN; Sita et al. 2022), cyanoacenaphthylene ($C_{12}H_7CN$; Cernicharo et al. 2024), cyanopyrene ($C_{16}H_9CN$; Wenzel et al. 2025b), and cyanocoronene ($C_{24}H_{11}CN$; Wenzel et al. 2025a). A key question is whether these aromatic species are formed in situ in dense molecular clouds through bottom-up chemical pathways, or whether they originate from the fragmentation of larger PAHs that are assumed to be present in the diffuse interstellar medium. Overall, PAHs are thought to be widespread throughout the interstellar medium, as inferred from ubiquitous infrared and optical and near-infrared spectral features (Mallo et al. 2025; Tielens 2008). Current chemical models predict the formation of aromatic compounds via bottom-up chemistry, starting from the elemental constituents of these environments, but with large uncertainties (Agúndez et al. 2025; Byrne et al. 2024; Goettl et al. 2025; McGuire et al. 2021). This chemistry is largely driven by ion–molecule reactions, as supported by experimental studies (Anicich et al. 2006; Anicich 2003; McEwan & Anicich 2007; McEwan et al. 1999), with the phenylium cation ($C_6H_5^+$) playing a central role (Loison et al. 2025). More recently, neutral–neutral reaction pathways have been proposed as alternative routes to aromatic formation Goettl et al. (2025); Jones et al. (2011); Kaiser et al. (2022); Yang et al. (2024b,a). While both ionic and neutral chemistries successfully reproduce the observed abundance of benzene in Titan's atmosphere (Loison et al. 2019; Vuitton et al. 2008), they fail to do so in dense molecular clouds,

⋆ Corresponding authors: jean-christophe.loison@cnrs.fr; ugo.jacovella@cnrs.fr

where current models underestimate the abundances of aromatic species by several orders of magnitude (Byrne et al. 2024; McGuire et al. 2021).

To better constrain the chemistry of aromatic species in the interstellar medium, we revisited aromatic formation pathways using an approach similar to that adopted in our previous reviews of Titan's chemistry (Dobrijevic et al. 2014, 2016; Hébrard et al. 2012, 2013; Loison et al. 2019, 2015), as well as in our recent work improving the chemical formation of cyclopentadiene in dense molecular clouds (Jacovella et al. 2026). We systematically examined reactions leading to the formation of the first C_6 aromatic species (C_6H_4, C_6H_5, $C_6H_5^+$, C_6H_6, $C_6H_6^+$, and $C_6H_7^+$), starting from species that have been detected or that exhibit significant modeled abundances, considering both ionic and neutral reaction pathways. With the updated chemical network, the observed abundances of C_6H_4, C_6H_5CN, and $C_6H_5C_2H$ can be reproduced, although they remain underestimated by approximately a factor of two. Our analysis highlights the critical role of l-$C_3H_3^+$ and CH_3CCH in the formation of aromatics. In particular, the production of the first aromatic species requires an accurate description of CH_3CCH chemistry, which is still poorly constrained in dense molecular clouds (Hickson et al. 2016b).

2. General methodology

To identify reactions leading to the formation of the first C_6 aromatic compounds, we systematically examined processes producing $C_6H_x^+$ species with $x \geq 5$ and neutral C_6H_y species with $y \geq 4$. Species reacting quickly with H_2, such as CH^+, CH_2^+, C_2^+, C_2H^+, and $C_2H_2^+$ (Anicich 2003), which exhibit very low abundances, were not considered because the fluxes of the reactions with the other species are very low. Reactions forming aromatic species containing more than six carbon atoms were not investigated systematically, although some were included in the chemical network. After compiling a list of potentially relevant reactions, a comprehensive literature survey was conducted for each reaction. When reaction rate coefficients have been measured, at least at room temperature, and exceed 10^{-11} cm^3 s^{-1}, the reactions were considered to be barrierless and, thus, efficient even under dense cloud conditions. However, for many reactions, no experimental or theoretical data are available. In such cases, priority was given to reactions that were expected to be rapid at low temperatures on the basis of the reactivity of the involved species. Highly reactive species (C, CH, C_2, and C_2H) are known to react without barrier with both radicals and closed-shell species (including alkanes in the case of CH and C_2) and most of their rate coefficients have been measured. In contrast, less reactive radicals such as CH_2, CH_3, and C_2H_3 typically react in a barrierless manner only with other radicals. A notable exception concerns reactions involving C_3. While C_3 does not react with atomic oxygen or nitrogen (Woon & Herbst 1996), while only reacting slowly with atomic carbon under interstellar conditions (Wakelam et al. 2009), it was shown by Mebel et al. (2023) to react without a barrier with carbon radicals such as C_3H_3. These reactions efficiently increase molecular size and must therefore be considered, although the presence or absence of barriers remains difficult to assess. To further evaluate the existence of activation barriers, we searched for transition states (TSs) using density functional theory (DFT) calculations performed with Gaussian16 (Frisch et al. 2016), employing the M06-2X functional with the aug-cc-pVTZ basis set. This highly nonlocal functional developed by Zhao & Truhlar (2008) is well suited for describing transition-state structures and energetics with an average errors on barrier heights calculated around 7 kJ/mol on 449 chemical reactions Prasad et al. (2022a,b). The absence of a TS, however, does not unequivocally demonstrate that a reaction is barrierless. For the reaction $C_3 + C_3H_5$, a potential source of C_6H_4, for which the absence of a barrier on the entrance pathway seemed ambiguous to us, we computed the interaction potentials as a function of the reactant separation to further assess the presence of barrier.

Ion–molecule reactions constitute another important class of processes potentially leading to aromatic formation. Despite the relatively low ion abundances imposed by electronic dissociative recombination (DR) reactions, ion–molecule reactions often proceed at high rates, especially with unsaturated species. When no direct data were available, ionic reactions were inferred by analogy with similar, well-characterized systems. For example, if an ion reacts efficiently with C_2H_2, it was assumed to react similarly with other alkynes such as C_3H^+ and $C_3H_2^+$ with C_2H_2, CH_2CCH_2, CH_3CCH and C_4H_2 (Anicich 2003), and analogous reasoning was applied to reactions with alkenes such as C_3H^+ and $C_3H_2^+$ with C_2H_4 and C_3H_6 (Anicich 2003). For ionic reactions involving H_2 or CH_4, where barriers are often present, explicit TS searches were performed for poorly constrained or ambiguous reactions. A particularly delicate aspect of this work concerns the identification of reaction products and branching ratios. When available, experimental studies were used; otherwise, theoretical investigations were considered. In the absence of both, additional DFT calculations were performed to characterize key intermediates and to estimate product distributions. Owing to the large number of atoms involved and the substantial internal energies, many reactions may proceed through a complex network of intermediates. Our approach does not aim to identify all possible pathways, as this would require detailed statistical treatments, as illustrated in the work of Mallo et al. (2025) on the l-$C_3H_3^+ + C_2H_4$ reaction. Instead, the goal is to determine whether cyclization and aromatic formation are feasible. Branching ratios remain particularly uncertain without comprehensive statistical calculations. For reactions producing a $C_6H_6^+$ isomer as an initial product and potentially constituting major sources of $C_6H_5^+$—such as $C_2H_4^+ + C_4H_2$, $C_3H_2^+ + C_3H_4$, l-$C_3H_3^+ + C_3H_3$, and $C_4H_2^+ + C_2H_4$—the rates and branching ratios were assumed to be similar to those measured for $C_4H_2^+ + C_2H_4$ by Anicich et al. (2006). The dependence of product distributions on internal energy was accounted for by comparison with $C_3H_2^+ + C_3H_4$ (Anicich et al. 1984) and with our recent experiments at SOLEIL (forthcoming publication).

DFT calculations are also essential for reactions that have been partially characterized experimentally but for which products are identified only by their masses. In many cases, several structural isomers may be formed and their identification is critical, as isomers often exhibit markedly different reactivities (e.g., l-$C_3H_3^+$ versus c-$C_3H_3^+$, or phenylium (c-$C_6H_5^+$) versus other $C_6H_5^+$ isomers) Kocheril et al. (2025); Loison et al. (2025). Although cyclic aromatic structures are thermodynamically favored, they are not necessarily formed preferentially, as illustrated by the $C_3H_3 + C_3H_3$ reaction (Hrodmarsson et al. 2024; Miller & Klippenstein 2003) and by $C_3H_2^+ + C_3H_4$ (Anicich et al. 1984) and examples given in this work. Finally, the estimation of branching ratios for DR reactions represents another major uncertainty. In the present network, aromatic formation predominantly proceeds through benzene production via the DR of $C_6H_7^+$. While direct measurements of branching ratios for the DR of aromatic ions are lacking, experimental studies of $C_6D_6^+$ and $C_6D_7^+$ by Hamberg et al. (2011) indicate that the

aromatic ring is preserved in more than 90% of cases. Accordingly, we assume that DR predominantly conserves the aromatic ring and that the reaction $C_6H_7^+ + e^-$ mainly yields C_6H_6.

3. Astrochemical modeling

The abundances of the various species present in dense molecular clouds were computed using the Nautilus astrochemical code (Ruaud et al. 2016). Nautilus is a three-phase, time-dependent chemical model that treats the gas phase, dust–grain ice surface, and dust–grain ice mantle. The chemical network is based on kida.uva.2024 (Wakelam et al. 2024), recently updated to improve the description of complex organic molecule (COM) chemistry on interstellar dust grains and in the gas phase (Coutens et al. 2022; Hickson et al. 2021, 2024; Manigand et al. 2021). It was further extended by the updated network presented in this work, including the review summarized in Appendix A. The resulting network includes approximately 800 chemical species involved in about 9000 reactions. All elements were initially assumed to be in either atomic or ionic form, while elements with ionization potentials lower than 13.6 eV were assumed to be fully ionized. The gas-phase elemental C/O ratio was set to unity. Although this value is higher than the cosmic abundance ratio (C/O $\simeq$ 0.6), it provides significantly better agreement between the model predictions and the full set of observations. For lower C/O ratios, an excess of oxygen leads to efficient CO formation, leaving insufficient carbon to sustain the radical-driven chemistry. The remaining oxygen atoms then strongly suppress the abundances of radicals, thereby inhibiting the overall chemical complexity. The choice of C/O = 1 is consistent with previous studies, including the O_2 investigation by Hincelin et al. (2011) and more recent studies of aromatic species and complex carbon chemistry (Byrne et al. 2024; Mallo et al. 2025; Jacovella et al. 2026; Byrne et al. 2026). From a physical standpoint, this process of oxygen depletion could be explained by the formation of water ice during earlier dense phases of cloud evolution. Water ice remains locked on grain surfaces during subsequent warmer and less dense phases, unlike CO, which can desorb and dissociate into atomic C and O Hincelin et al. (2016); Ruaud et al. (2018); Wakelam et al. (2019). The physical conditions adopted in the model are representative of dense molecular clouds: a total hydrogen density (n_{tot}(H)= n(H) + 2n(H_2)) of 5.0×10^4 cm^{-3}, temperature of 10 K, cosmic-ray ionization rate of 1.3×10^{-17} s^{-1}, and visual extinction of A_V = 10. The initial elemental abundances are listed in Table 1.

In these simulations, both the grain surface and the ice mantle are treated as chemically active, whereas accretion and desorption processes are permitted only between the grain surface and the gas phase. A dust-to-gas mass ratio of 0.01 is adopted. A sticking probability of unity is assumed for all neutral species. Desorption proceeds via thermal and non-thermal mechanisms, including cosmic-ray–induced desorption, chemical desorption, and ice sputtering by cosmic-ray collisions (Wakelam et al. 2021). A detailed description of the surface reaction formalism and the simulation methodology is provided by Ruaud et al. (2016).

4. Results

The modeled abundances, together with observed abundances when available, of the species involved in the potential formation pathways of aromatic C_6 compounds are shown in Fig. 1. The calculated abundances indicate that among carbon-based radical species, atomic carbon is by far the most abundant and therefore the most efficient driver of molecular size growth. Radicals such as CH, C_2, and C_2H can react with closed-shell species; however, their abundances are low, and the associated reaction fluxes are generally small. Nevertheless, these reactions have been included in our chemical network and may become relevant when the reactant molecules are particularly abundant. Less reactive radicals, including CH_2, CH_3, C_2H_3, C_3H_3, C_3H_5, and C_4H_3, react without activation barriers only with other radicals. Given their low abundances, the resulting radical–radical reaction fluxes are weak, and these processes play only a minor role in the chemistry. However, they have been retained in the network for completeness. In contrast to carbon radicals, the ions of interest are partially hydrogenated and carry multiple hydrogen atoms. Reactions involving such species allow for the formation of molecules with a high hydrogen content, which is generally otherwise inaccessible through reactions involving bare carbon radicals. In this context, ions such as $C_2H_4^+$, (l,c)–$C_3H_2^+$, l-$C_3H_3^+$, $C_3H_5^+$, and $C_4H_3^+$ emerge as promising candidates for the formation of the first aromatic compounds.

Table 1. Elemental abundances.

Element	Abundance[(a)]
H_2	0.5
He	0.09
C^+	1.4×10^{-4}
N	3.0×10^{-5}
O	1.4×10^{-4}
s-H_2O[(b)]	1.0×10^{-4}
S^+	4.0×10^{-6}
Fe^+	2.0×10^{-8}
Cl^+	1.0×10^{-7}
F	6.7×10^{-9}

Notes. [(a)] Relative to total hydrogen (n(H) + 2n(H_2)). [(b)] s–H_2O means H_2O on grain.

Main aromatic formation reactions

An analysis of the reaction fluxes leading to the formation of the first aromatic species is presented in Fig. 2, where the widths of the arrows are proportional to the corresponding reaction fluxes. This analysis enables the identification of the dominant production pathways. The three most significant reactions are:

- l-$C_3H_3^+$ + C_3H_4 (followed by $C_6H_5^+$ + H_2, then $C_6H_7^+$ + e^-), which accounts for approximately 60% of the total production of C_6H_6;
- l-$C_3H_5^+$ + C_3H_4 (followed by $C_6H_7^+$ + e^-), which accounts for approximately 15% of the total production of C_6H_6;
- C + c-C_5H_6 (followed by C_6H_5 + H), which accounts for approximately 10% of the total production of C_6H_6.

The remaining 15% arise from secondary $C_6H_5^+$ formation pathways. Although these reactions remain uncertain, particularly at the low temperatures of dense interstellar clouds, the rates and branching ratios of the dominant reactions are relatively well constrained at room temperature (Appendix A). Several species involved in aromatic formation (l-$C_3H_3^+$, CH_3CCH, c-C_5H_6) have been observed. For l-$C_3H_3^+$ and CH_3CCH, the modeled abundances agree well with observations, providing further validation of the C_6H_6 production pathways. However, since the

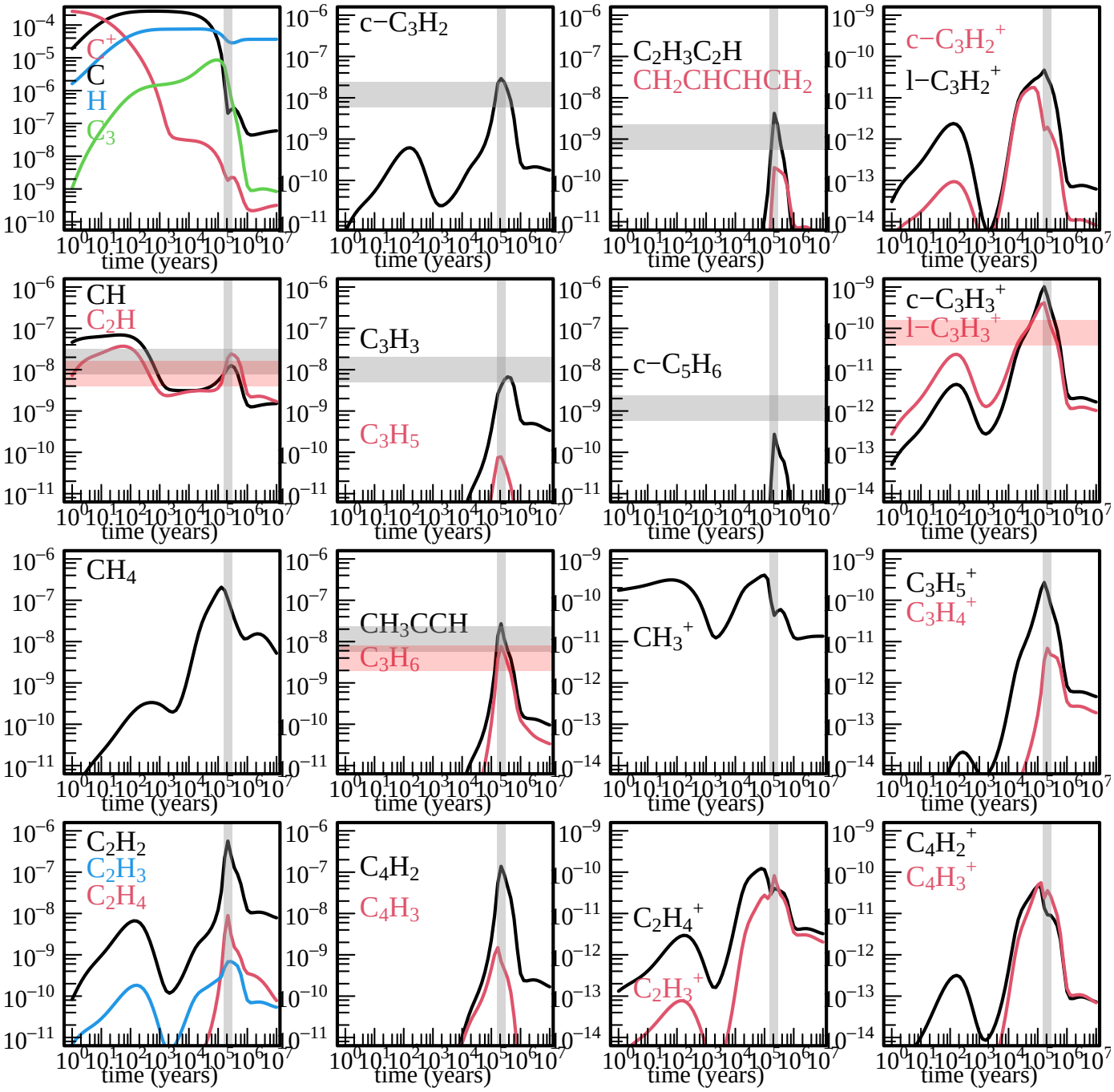

Fig. 1. Gas–grain astrochemical model results for the calculated abundances (relative to H_2) of the most important species involved in the formation of aromatic molecules in dark clouds, shown as a function of cloud age. The horizontal gray region represent the observed abundances in TMC-1, with an arbitrary uncertainty of plus or minus a factor of 2: CH (Suutarinen et al. 2011), C_2H (Sakai et al. 2010; Turner et al. 2000), c-C_3H_2 (Park et al. 2006; Turner et al. 2000), l-$C_3H_3^+$ (Silva et al. 2023), CH_3CCH (Askne et al. 1983; Irvine et al. 1981; Markwick et al. 2002; Turner et al. 1999), C_3H_6 (Marcelino et al. 2007), and c-C_5H_6 (Cernicharo et al. 2021a). The vertical gray region indicates the chemical age obtained by minimizing the distance of disagreement (Wakelam et al. 2006), which in this study involves the differences between the observed and modeled abundances of 62 species in TMC-1.

abundance of c-C_5H_6 is underestimated by a factor of ≈ 6, the C + c-C_5H_6 pathway (leading to c-C_6H_5 + H) is likely underestimated as well.

In Fig. 3, we compare the nominal model with the observed abundances of C_6H_4, C_6H_5CN, and $C_6H_5C_2H$. The agreement is generally good, although the model underestimates the abundances by approximately a factor of two. We also show (in red) the results from a model excluding the $C_6H_5^+ + H_2$ reaction, which constitutes the primary formation pathway of $C_6H_7^+$ (≈ 85%). Omitting this reaction leads to a substantial decrease in aromatic abundances by roughly a factor of five, highlighting its importance; in addition, it also contextualizes its critical role when the chemical network is completed Loison et al. (2025). Interestingly, in the absence of this reaction, the modeled abundance of C_6H_4 increases significantly. This is because, without $C_6H_5^+ + H_2$, the DR of $C_6H_5^+$, which

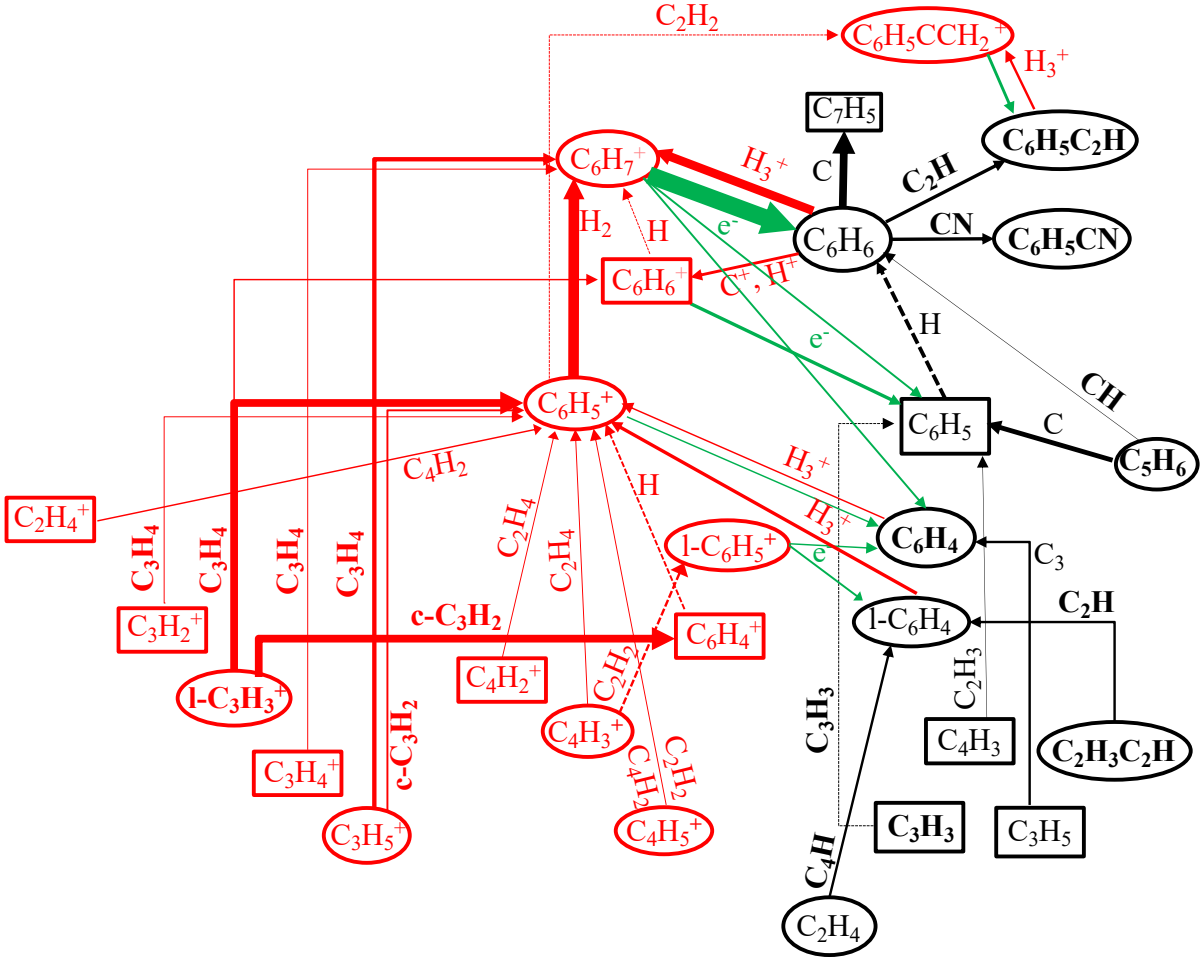

Fig. 2. Schematic diagram of the main neutral (black) and ionic (red or green for dissociative recombination, DR) pathways leading to the formation of aromatic species. Most DRs, typically represent the major destruction pathways for ions, are not shown because they generally do not lead to the formation of aromatic cycles. Arrow widths are proportional to the integrated total production rates. Radiative association reactions are indicated by dashed lines. Radicals are shown in boxes, and closed-shell species in circles. Observed species in TMC-1 (C_3H_3, l-$C_3H_3^+$, C_6H_5CN, $C_6H_5C_2H$, etc.) are highlighted in bold.

produces C_6H_4 in our network, becomes the dominant consumption pathway of $C_6H_5^+$.

When the $C_6H_5^+ + H_2$ reaction is included, the DR of $C_6H_5^+$ only contributes a minor flux. The main production pathways for C_6H_4 are $C_3 + C_3H_5$ (this work) and $C_6H_7^+ + e^-$. Notably, the formation of linear l-C_6H_4 isomers (sum of species e.g., $C_2H_3C_4H$, CHCCHCHCCH, etc.) via reactions such as $C_2H + C_2H_3C_4H$ and $C_4H + C_2H_4$ involves higher fluxes than the production of benzyne. This suggests that some of these linear isomers may be detectable. If the DR of $C_6H_7^+$ were assumed to produce only C_6H_6, the calculated C_6H_4 abundance would decrease by ≈40%, yet it would still remain in good agreement with observations, highlighting the importance of the $C_3 + C_3H_5$ pathway. This change has little impact on the abundances of C_6H_6 and other aromatic species.

A crucial aspect in the formation of the first C_6 aromatic compounds is the role of neutral and ionic C_3 species (C_3, C_3H_3, l-$C_3H_3^+$, CH_3CCH, CH_2CCH_2, $C_3H_5^+$). Several of these species have been detected in TMC-1 (C_3H^+, l-C_3H, c-C_3H, l-C_3H_2, c-C_3H_2, C_3H_3, l-$C_3H_3^+$, CH_3CCH, and C_3H_6), but reproducing the abundances of CH_3CCH and C_3H_6 in models is challenging. While the chemistry of C_3 species is well understood up to the formation of (c,l)−$C_3H_3^+$ (Hickson et al. 2016b; Loison et al. 2017), processes beyond this point remain uncertain. In particular, the reactions (c,l)−$C_3H_3^+ + H_2$ and $C_3H_5^+ + H_2$ have a barrier in the entrance valley (Lin et al. 2013), which limits the formation of $C_3H_5^+$ and $C_3H_7^+$, the main gas-phase precursors of C_3H_4 and C_3H_6 (alternative pathways, e.g., $CH + C_2H_4$, contribute much smaller fluxes). Grain-surface chemistry provides a non-negligible source of C_3H_4 and C_3H_6, but it is insufficient to match the observed abundances (Hickson et al. 2016b).

To reproduce the observed abundances of CH_3CCH, we chose to use (without including any theoretical calculations) a low but non-negligible set of rates for l-$C_3H_3^+ + H_2$, consistent with the 300 K upper limits and the calculated energy barriers (Savić & Gerlich 2005; Lin et al. 2013). Under these conditions, $C_3H_5^+$ could be formed via quantum tunneling, analogous to the $C_2H_2^+ + H_2$ reaction (Hawley & Smith 1989, 1992), $NH_3^+ + H_2$ reaction (Herbst et al. 1991), $OH + CH_3OH$ reaction (Shannon et al. 2013) and $C + H_2O$ reaction (Hickson et al. 2016a). These reactions exhibit a sharply increasing rate at low temperatures despite the presence of an activation barrier. This increase can be interpreted based on the formation of a hydrogen-bonded complex that is sufficiently long-lived to undergo quantum-mechanical tunnelling to form products as explained in Shannon et al. (2013). Without this reaction, the

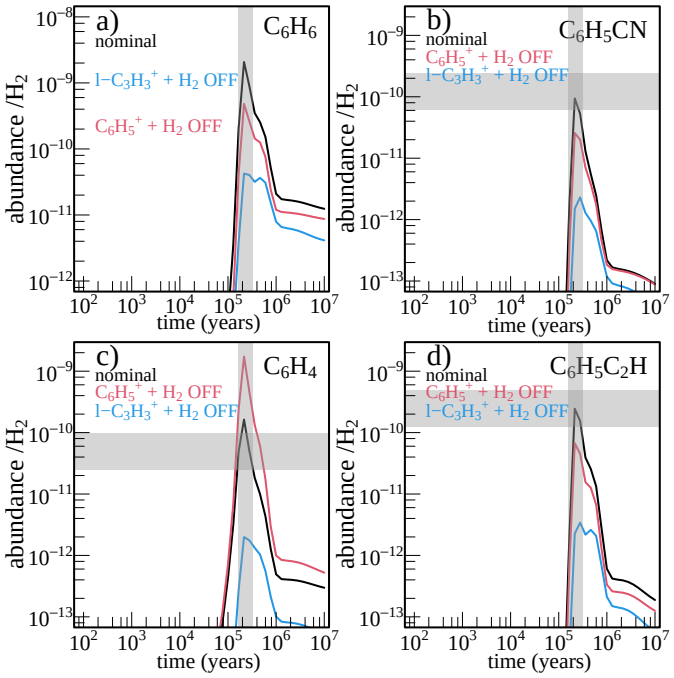

Fig. 3. Gas–grain astrochemical model results for l-$C_3H_3^+$, CH_3CCH, C_6H_4, C_6H_6, C_6H_5CN, and $C_6H_5C_2H$ in dark clouds as a function of cloud age. Solid black line: standard network results. Solid red line: nominal network excluding the gas-phase $C_6H_5^+ + H_2$ reaction. Solid blue line: nominal network excluding the gas-phase l-$C_3H_3^+ + H_2$ reaction. Horizontal shaded rectangle: observed abundances in TMC-1 with an arbitrary error of ±2: l-$C_3H_3^+$ Silva et al. (2023), CH_3CCH (Askne et al. 1983; Irvine et al. 1981; Markwick et al. 2002; Turner et al. 1999), C_6H_4 Cernicharo et al. (2021b), C_6H_5CN McGuire et al. (2018), and $C_6H_5C_2H$ (Loru et al. 2023).

model fails to reproduce the observed abundances of CH_3CCH and then the aromatic species as CH_3CCH ends up being involved in the main aromatic pathways formation, with predicted abundances of CH_3CCH, C_6H_4, C_6H_5CN, and $C_6H_5C_2H$ being roughly 100 times lower than observed (blue line in Fig. 3). Introducing this reaction also enables the reproduction of species derived from CH_3CCH and CH_2CCH_2, such as $C_2H_3C_2H$ (produced by CH + CH_2CCH_2 and CH + CH_3CCH) and CH_3C_4H (produced by C_2H + CH_3CCH). It does not otherwise disrupt the rest of the network. Indeed, all species are at least as well described, including c-C_3H_2 produced by the electronic recombination of c-$C_3H_3^+$, which is found not to react with H_2, even at low temperatures.

5. Conclusions

We performed a systematic survey of the chemical network leading to the formation of the first aromatic compounds in dense molecular clouds, with a particular focus on reactions producing C_6H_x ($x \geq 4$) species. By reassessing both ionic and neutral pathways and incorporating updated experimental and theoretical constraints, we identified a limited number of key reactions that dominate the formation of C_6 aromatic species under typical dense-cloud conditions.

Our results show that the observed abundances of C_6H_4, C_6H_5CN, and $C_6H_5C_2H$ in TMC-1 can be reproduced when the chemistry of C_3 species is treated consistently. In particular, ionic reactions involving l-$C_3H_3^+$ and l-$C_3H_5^+$ with C_3H_4, together with the neutral reaction C + c-C_5H_6, emerge as the dominant contributors to the formation of the first aromatic ring. These results highlight the central role of both neutral and ionic C_3 chemistry, which remains one of the main sources of uncertainty in current astrochemical models.

Despite these improvements, significant uncertainties persist, especially regarding the formation and destruction pathways of CH_3CCH, $C_3H_5^+$ and c-C_5H_6, which strongly influence the overall efficiency of aromatic formation. Further laboratory measurements and theoretical studies of these key reactions at low temperatures are therefore required. Extending the present approach to larger aromatic systems will be essential for assessing whether a bottom-up gas-phase chemistry is sufficient to account for the formation of more complex polycyclic aromatic hydrocarbons in dense molecular clouds.

Acknowledgements. The work was funded by the French "Agence Nationale de la Recherche" (ANR) under grant no. ANR-22-CE29-0013 (Project iSELECTION).This work was also supported by the Programme National "Physique et Chimie du Milieu Interstellaire" (PCMI) and a research grant (VIL71404) from VILLUM FONDEN.

References

Ackermann, L., Hippler, H., Pagsberg, P., Reihs, C., & Troe, J. 1990, J. Phys. Chem., 94, 5247
Agúndez, M., Cabezas, C., Marcelino, N., et al. 2025, A&A, 697, A82
Anicich, V. G. 2003, JPL Publication-03-19, Pasadena, CA, USA
Anicich, V. G., Blake, G. A., Kim, J. K., McEwan, M. J., & Huntress, Wesley T., J. 1984, J. Phys. Chem., 88, 4608
Anicich, V. G., Wilson, P., & McEwan, M. J. 2003, J. Am. Chem. Soc. Mass Spectrom., 14, 900
Anicich, V. G., Wilson, P. F., & McEwan, M. J. 2006, J. Am. Chem. Soc. Mass. Spectrom., 17, 544
Askne, J., Höglund, B., Hjalmarson, A., & Irvine, W. M. 1983, A&A, 130, 311
Ausloos, P., Lias, S. G., Buckley, T. J., & Rogers, E. E. 1989, Int. J. Mass Spectrom. Ion Processes, 92, 65
Baulch, D. L., Cobos, C. J., Cox, R. A., et al. 1994, J. Phys. Chem. Ref. Data, 23, 847
Bergeat, A., & Loison, J.-C. 2001, Phys. Chem. Chem. Phys., 3, 2038
Berman, M. R., Fleming, J. W., Harvey, A. B., & Lin, M. C. 1982, Chem. Phys., 73, 27
Berteloite, C., Le Picard, S. D., Balucani, N., Canosa, A., & Sims, I. R. 2010, Phys. Chem. Chem. Phys., 12, 3677
Betts, N. B., Stepanovic, M., Snow, T. P., & Bierbaum, V. M. 2006, ApJ, 651, L129
Bohme, D. K., Rakshit, A. B., & Schiff, H. I. 1982, Chem. Phys. Lett., 93, 592
Burkhardt, A. M., Long Kelvin Lee, K., Bryan Changala, P., et al. 2021, ApJ, 913, L18
Byrne, A. N., Xue, C., Van Voorhis, T., & McGuire, B. A. 2024, Phys. Chem. Chem. Phys., 26, 26734
Byrne, A. N., Shingledecker, C. N., Bergin, E. A., et al. 2026, ApJ, 998, 95
Caster, K. L., Selby, T. M., Osborn, D. L., Le Picard, S. D., & Goulay, F. 2021, J. Phys. Chem. A, 125, 6927
Castiñeira Reis, M., Martínez Núñez, E., & Fernández Ramos, A. 2024, Sci. Adv., 10, eadq4077
Cernicharo, J., Agúndez, M., Cabezas, C., et al. 2021a, A&A, 649, L15
Cernicharo, J., Agúndez, M., Kaiser, R. I., et al. 2021b, A&A, 652, L9
Cernicharo, J., Fuentetaja, R., Agúndez, M., et al. 2022, A&A, 663, L9
Cernicharo, J., Cabezas, C., Fuentetaja, R., et al. 2024, A&A, 690, L13
Coutens, A., Loison, J.-C., Boulanger, A., et al. 2022, A&A, 660, L6
da Silva, G. 2014, J. Phys. Chem. A, 118, 3967
Dobrijevic, M., Hébrard, E., Loison, J., & Hickson, K. 2014, Icarus, 228, 324
Dobrijevic, M., Loison, J., Hickson, K., & Gronoff, G. 2016, Icarus, 268, 313
Duran, R. P., Amorebieta, V. T., & Colussi, A. J. 1988, J. Phys. Chem., 92, 636
Fournier, J. A., Shuman, N. S., Melko, J. J., Ard, S. G., & Viggiano, A. A. 2013, J. Chem. Phys., 138
Frank, P., Herzler, J., Just, T., & Wahl, C. 1994, Symposium (International) on Combustion, 25, 833
Frisch, M. J., Trucks, G. W., Schlegel, H. B., et al. 2016, Gaussian~16 Revision C.01, Gaussian Inc., Wallingford, CT
Georgievskii, Y., & Klippenstein, S. J. 2005, J. Chem. Phys., 122, 194103
Georgievskii, Y., Miller, J. A., & Klippenstein, S. J. 2007, Phys. Chem. Chem. Phys., 9, 4259
Goettl, S. J., Turner, A. M., Krasnoukhov, V. S., et al. 2025, Sci. Adv., 11, eadv0692

Goulay, F., & Leone, S. R. 2006, J. Phys. Chem. A, 110, 1875
Hahndorf, I., Lee, Y. T., Kaiser, R. I., et al. 2002, J. Chem. Phys., 116, 3248
Haider, N., & Husain, D. 1993a, Berichte Bunseng. Phys. Chem., 97, 571
Haider, N., & Husain, D. 1993b, Int. J. Chem. Kinet., 25, 423
Hamberg, M., Vigren, E., Thomas, R., et al. 2011, EAS, 46, 241
Harrison, A. G. 1963, Can. J. Chem., 41, 236
Hawley, M., & Smith, M. A. 1989, J. Am. Chem. Soc., 111, 8293
Hawley, M., & Smith, M. A. 1992, J. Chem. Phys., 96, 1121
Hébrard, E., Dobrijevic, M., Loison, J.-C., Bergeat, A., & Hickson, K. 2012, A&As, 541, A21
Hébrard, E., Dobrijevic, M., Loison, J.-C., et al. 2013, A&A, 552, A132
Herbst, E., DeFrees, D. J., Talbi, D., et al. 1991, J. Chem. Phys., 94, 7842
Herbst, E., Terzieva, R., & Talbi, D. 2000, MNRAS, 311, 869
Hickson, K. M., Loison, J.-C., Nuñez-Reyes, D., & Méreau, R. 2016a, J. Phys. Chem. Lett., 7, 3641
Hickson, K. M., Wakelam, V., & Loison, J.-C. 2016b, Mol. Astrophys., 3, 1
Hickson, K. M., Loison, J.-C., & Wakelam, V. 2021, ACS Earth Space Chem., 5, 824
Hickson, K. M., Loison, J.-C., & Wakelam, V. 2024, ACS Earth Space Chem., 8, 1087
Hincelin, U., Wakelam, V., Hersant, F., et al. 2011, A&A, 530, A61
Hincelin, U., Commerçon, B., Wakelam, V., et al. 2016, ApJ, 822, 12
Hrodmarsson, H. R., Garcia, G. A., Bourehil, L., et al. 2024, Commun. Chem., 7, 156
Irvine, W. M., Hoglund, B., Friberg, P., Askne, J., & Ellder, J. 1981, ApJ, 248, L113
Jacovella, U., Loison, J.-C., Rossi, C., et al. 2026, A&A, 708, A281
Jones, B. M., Zhang, F., Kaiser, R. I., et al. 2011, PNAS, 108, 452
Kaiser, R. I., Hahndorf, I., Huang, L. C. L., et al. 1999, J. Chem. Phys., 110, 6091
Kaiser, R. I., Zhao, L., Lu, W., et al. 2022, J. Phys. Chem. Lett., 13, 208
Keheyan, Y. 2001, Chem. Phys. Lett., 340, 405
Knight, J. S., Freeman, C. G., McEwan, M. J., Anicich, V. G., & Huntress, W. T. 1987, J. Phys. Chem., 91, 3898
Kocheril, G., Zagorec-Marks, C., & Lewandowski, H. 2025, Nat. Astron., 1
Landera, A., Krishtal, S. P., Kislov, V. V., Mebel, A. M., & Kaiser, R. I. 2008, J. Chem. Phys., 128
Lee, K. L. K., McGuire, B. A., & McCarthy, M. C. 2019, Phys. Chem. Chem. Phys., 21, 2946
Lin, Z., Talbi, D., Roueff, E., et al. 2013, ApJ, 765, 80
Loison, J., Hébrard, E., Dobrijevic, M., et al. 2015, Icarus, 247, 218
Loison, J.-C., Agúndez, M., Wakelam, V., et al. 2017, MNRAS, 470, 4075
Loison, J., Dobrijevic, M., & Hickson, K. 2019, Icarus, 329, 55
Loison, J.-C., Rossi, C., Solem, N., et al. 2025, arXiv e-prints [arXiv:2506.13290]
Loru, D., Cabezas, C., Cernicharo, J., Schnell, M., & Steber, A. L. 2023, A&A, 677, A166
Madden, L. K., Moskaleva, L. V., Kristyan, S., & Lin, M. C. 1997, J. Phys. Chem. A, 101, 6790
Mallo, M., Agúndez, M., Cernicharo, J., & Molpeceres, G. 2025, A&A, 704, A249
Manigand, S., Coutens, A., Loison, J.-C., et al. 2021, A&A, 645, A53
Marcelino, N., Cernicharo, J., Agundez, M., et al. 2007, ApJ, 665, L127
Markwick, A. J., Millar, T. J., & Charnley, S. B. 2002, A&A, 381, 560
McCarthy, M. C., Lee, K. L. K., Loomis, R. A., et al. 2021, Nat. Astron., 5, 176
McEwan, M. J., & Anicich, V. G. 2007, Mass Spectrom. Rev., 26, 281
McEwan, Murray, J., Scott, Graham, B. I., Adams, Nigel, G., et al. 1999, ApJ, 513, 287
McGuire, B. A., Burkhardt, A. M., Kalenskii, S., et al. 2018, Science, 359, 202
McGuire, B. A., Loomis, R. A., Burkhardt, A. M., et al. 2021, Science, 371, 1265
Mebel, A. M., Agúndez, M., Cernicharo, J., & Kaiser, R. I. 2023, ApJ, 945, L40
Miller, J. A., & Klippenstein, S. J. 2003, J. Phys. Chem. A, 107, 7783
Milligan, D. B., Wilson, P. F., Freeman, C. G., Meot-Ner, M., & McEwan, M. J. 2002, J. Phys. Chem. A, 106, 9745
Ozturk, F., Moini, M., Brill, F. W., et al. 1989, J. Phys. Chem., 93, 4038
Park, I. H., Wakelam, V., & Herbst, E. 2006, A&A, 449, 631
Petrie, S., Javahery, G., & Bohme, D. K. 1992, J. Am. Chem. Soc., 114, 9205
Peverati, R., Bera, P. P., Lee, T. J., & Head-Gordon, M. 2016, ApJ, 830, 128
Prasad, V. K., Pei, Z., Edelmann, S., Otero-de-la Roza, A., & DiLabio, G. A. 2022a, J. Chem. Theory Comput., 18, 151
Prasad, V. K., Pei, Z., Edelmann, S., Otero-de-la Roza, A., & DiLabio, G. A. 2022b, J. Chem. Theory Comput., 18, 4041
Prodnuk, S. D., Grocert, S., Bierbaum, V. M., & DePuy, C. H. 1992, Org. Mass Spectrom., 27, 416
Ruaud, M., Wakelam, V., & Hersant, F. 2016, MNRAS, 459, 3756
Ruaud, M., Wakelam, V., Gratier, P., & Bonnell, I. 2018, A&A, 611, A96
Sakai, N., Saruwatari, O., Sakai, T., Takano, S., & Yamamoto, S. 2010, A&A, 512, A31
Savić, I., & Gerlich, D. 2005, Phys. Chem. Chem. Phys., 7, 1026
Scott, G. B. I., Fairley, D. A., Freeman, C. G., et al. 1997, J. Phys. Chem. A, 101, 4973
Scott, G. B. I., Milligan, D. B., Fairley, D. A., Freeman, C. G., & McEwan, M. J. 2000, J. Chem. Phys., 112, 4959
Shannon, R. J., Blitz, M. A., Goddard, A., & Heard, D. E. 2013, Nat. Chem., 5, 745
Silva, W. G. D. P., Cernicharo, J., Schlemmer, S., et al. 2023, A&A, 676, L1
Sita, M. L., Changala, P. B., Xue, C., et al. 2022, Astrophys. J. Lett., 938, L12
Smith, R. D., & Futrell, J. H. 1978, Int. J. Mass Spectrom. Ion Phys., 26, 111
Snow, T. P., Le Page, V., Keheyan, Y., & Bierbaum, V. M. 1998, Nature, 391, 259
Stranges, D., O'Keeffe, P., Scotti, G., Di Santo, R., & Houston, P. L. 2008, J. Chem. Phys., 128, 151101
Suutarinen, A., Geppert, W. D., Harju, J., et al. 2011, A&A, 531, A121
Tielens, A. 2008, Annu. Rev. Astron. Astrophys., 46, 289
Trevitt, A. J., Goulay, F., Taatjes, C. A., Osborn, D. L., & Leone, S. R. 2009, J. Phys. Chem. A, 114, 1749
Tseng, C.-M., Choi, Y. M., Huang, C.-L., et al. 2004, J. Phys. Chem. A, 108, 7928
Turner, B. E., Terzieva, R., & Eric, H. 1999, ApJ, 518, 699
Turner, B. E., Herbst, E., & Terzieva, R. 2000, ApJS, 126, 427
Vuitton, V., Yelle, R. V., & Cui, J. 2008, J. Geophys. Res., 113, E05007
Vuitton, V., Yelle, R. V., Lavvas, P., & Klippenstein, S. J. 2012, ApJ, 744, 11
Vuitton, V., Yelle, R. V., Klippenstein, S. J., Hörst, S. M., & Lavvas, P. 2019, Icarus, 324, 120
Wakelam, V., Herbst, E., & Selsis, F. 2006, A&A, 451, 551
Wakelam, V., Loison, J. C., Herbst, E., et al. 2009, A&A, 495, 513
Wakelam, V., Ruaud, M., Gratier, P., & Bonnell, I. 2019, MNRAS, 486, 4198
Wakelam, V., Dartois, E., Chabot, M., et al. 2021, A&A, 652, A63
Wakelam, V., Gratier, P., Loison, J.-C., et al. 2024, A&A, 689, A63
Wenzel, G., Gong, S., Xue, C., et al. 2025a, Astrophys. J. Lett., 984, L36
Wenzel, G., Speak, T. H., Changala, P. B., et al. 2025b, Nat. Astron., 9, 262
Woon, D. E. 2006, Chem. Phys., 331, 67
Woon, D. E., & Herbst, E. 1996, ApJ, 465, 795
Yang, Z., He, C., Goettl, S. J., et al. 2024a, Nat. Astron., 8, 856
Yang, Z., Medvedkov, I. A., Goettl, S. J., et al. 2024b, Proc. Natl. Acad. Sci., 121, e2409933121
Zhang, F., Parker, D., Kim, Y. S., Kaiser, R. I., & Mebel, A. M. 2011, ApJ, 728, 141
Zhao, Y., & Truhlar, D. G. 2008, Theor. Chem. Acc., 120, 215
Zyubina, T. S., Mebel, A. M., Hayashi, M., & Lin, S. H. 2008, Phys. Chem. Chem. Phys., 10, 2321

Appendix A: Chemical network for the production of benzene and its derivatives

Table A.1. Chemical network relevant for benzene formation. Rate coefficients $\alpha(T/300)^{\beta}\exp(-\gamma/T)$ are in units of $cm^3\ s^{-1}$. ΔH_R in kJ mol^{-1}. Reactions highlighted in grey such as 10 are not included in the network.

#	Reaction	ΔH_R	α	β	γ	ref
1	$H_3^+ + c\text{-}C_6H_4 \rightarrow c\text{-}C_6H_5^+ + H_2$	-442	4.0E-09	-0.15	0	Calculated using capture rate theory Georgievskii & Klippenstein (2005)
2	$H_3^+ + l\text{-}C_6H_4 \rightarrow c\text{-}C_6H_5^+ + H_2$	-472	4.1E-09	-0.22	0	[a]
	$l\text{-}C_6H_5^+ + H_2$	-371	0			
3	$H_3^+ + c\text{-}C_6H_5 \rightarrow c\text{-}C_6H_6^+ + H_2$	-451	4.4E-09	-0.26	0	Calculated using capture rate theory Georgievskii & Klippenstein (2005)
4	$H_3^+ + c\text{-}C_6H_6 \rightarrow c\text{-}C_6H_7^+ + H_2$	-311	3.9E-09	0	0	Milligan et al. (2002)
5	$H_3^+ + l\text{-}C_6H_6 \rightarrow c\text{-}C_6H_7^+ + H_2$	-572	5.0E-09	-0.22	0	[b]
6	$H_3^+ + c\text{-}C_7H_5 \rightarrow c\text{-}C_6H_6^+ + CH_2$	-257	4.1E-09	-0.10	0	Calculated using capture rate theory Georgievskii & Klippenstein (2005)
7	$H_3^+ + C_6H_5C_2H \rightarrow C_6H_5CCH_2^+ + H_2$	-400	4.8E-09	-0.10	0	Calculated using capture rate theory Georgievskii & Klippenstein (2005)
8	$H_3^+ + C_6H_5CN \rightarrow C_6H_5CNH^+ + H_2$	-382	1.1E-08	-0.44	0	Calculated using capture rate theory Georgievskii & Klippenstein (2005)
9	$C^+ + c\text{-}C_6H_6 \rightarrow C + c\text{-}C_6H_6^+$	-203	1.61E-09	0	0	Bohme et al. (1982); Smith & Futrell (1978)
	$c\text{-}C_7H_5^+ + H$	-546	2.40E-10	0	0	
	$l\text{-}C_5H_3^+ + C_2H_3$	-242	4.08E-10	0	0	
	$l\text{-}C_3H_3^+ + C_4H_3$	-212	1.44E-10	0	0	
10	$CH_3^+ + c\text{-}C_5H_6 \rightarrow c\text{-}C_6H_7^+ + H_2$	Cyclization of the first intermediate does not induce the formation of an aromatic ring and is therefore not favored thermodynamically and is unfavored kinetically.				
11	$C_2H_3^+ + C_4H_3 \rightarrow c\text{-}C_6H_5^+ + H$	Cyclization of the first intermediate does induce the formation of an aromatic ring. So it is a potential but secondary pathway for the production of $C_6H_5^+$ because C_4H_3 is expected to have a relatively low abundance. This reaction is not considered in this study.				
12	$C_2H_3^+ + C_2H_3C_2H \rightarrow c\text{-}C_6H_6^+ + H$	-213	0			[c]
	$c\text{-}C_6H_5^+ + H_2$	-275	5.0E-10	-0.5	0	
	$C_4H_5^+(c\text{-}C_3H_2CH_3^+) + C_2H_2$	-211	5.0E-10	-0.5	0	
13	$C_2H_3^+ + CH_2CHCHCH_2 \rightarrow c\text{-}C_6H_7^+ + H_2$	Cyclization of the first intermediate does not induce the formation of an aromatic ring and is therefore not favored thermodynamically and is unfavored kinetically.				
14	$C_2H_4^+ + C_4H_2 \rightarrow c\text{-}C_4H_4CCH^+ + H$	-55	1.0E-10	0	0	[d]
	$c\text{-}C_6H_5^+ + H$	-164	5.0E-10	0	0	
	$m\text{-}C_6H_4^+ + H_2$	-168	1.0E-11	0	0	
	$C_4H_4^+(c\text{-}C_3H_2CH_2^+) + C_2H_2$	-134	8.0E-10	0	0	
15	$C_2H_4^+ + C_2H_3C_2H \rightarrow c\text{-}C_6H_7^+ + H$	Potential secondary source of aromatic species. To be studied in the future.				
16	$c\text{-}C_3H_2^+ + C_3H_3 \rightarrow c\text{-}C_3H_2CHCCH^+ + H$	-155	1.0E-09	0	0	[e] Estimated using using Peverati et al. (2016).
17	$l\text{-}C_3H_2^+ + C_3H_3 \rightarrow c\text{-}C_6H_4^+ + H$	-206	5.0E-10	0	0	[e] Estimated using using
	$HCCCHCHCCH^+ + H$	-164	5.0E-10	0	0	Peverati et al. (2016).

Table A.1. continued.

#	Reaction	ΔH_R	α	β	γ	ref
18	c-$C_3H_2^+$ + CH_3CCH → c-$C_6H_5^+$ + H	-198	8.0E-11	-0.5	0	[e] Anicich et al. (1984) and new experiment at the SOLEIL synchrotron using the CERISES setup (in preparation)
	c-$C_3H_2CCH^+$ + CH_3	-123	1.0E-10	-0.5	0	
	$CH_2CCCH_2^+$ + C_2H_2	-121	5.0E-10	-0.5	0	
	$C_4H_3^+$ + C_2H_3	+19	0			
	$C_4H_2^+$ + C_2H_4	-53	1.7E-10	-0.5	0	
	c-$C_3H_3^+$ + C_3H_3	-139	4.0E-10	-0.5	0	
19	l-$C_3H_2^+$ + CH_3CCH → c-$C_6H_5^+$ + H	-254	8.0E-11	-0.5	0	[e] Anicich et al. (1984) and new experiment at the SOLEIL synchrotron using the CERISES setup (in preparation)
	c-$C_3H_2CCH^+$ + CH_3	-178	1.0E-10	-0.5	0	
	$CH_2CCCH_2^+$ + C_2H_2	-176	5.0E-10	-0.5	0	
	$C_4H_3^+$ + C_2H_3	-36	4.0E-11	-0.5	0	
	$C_4H_2^+$ + C_2H_4	-108	1.7E-10	-0.5	0	
	c-$C_3H_3^+$ + C_3H_3	-195	5.0E-10	-0.5	0	
20	c-$C_3H_2^+$ + CH_2CCH_2 → c-$C_6H_5^+$ + H	-198	6.0E-11	0	0	[e] Anicich et al. (1984) and new experiment at the SOLEIL synchrotron using the CERISES setup (in preparation)
	c-$C_3H_2CCH^+$ + CH_3	-123	1.2E-10	0	0	
	$CH_2CCCH_2^+$ + C_2H_2	-121	5.8E-10	0	0	
	$C_4H_3^+$ + C_2H_3	+19	0			
	$C_4H_2^+$ + C_2H_4	-53	1.0E-10	0	0	
	c-$C_3H_3^+$ + C_3H_3	-139	3.2E-10	0	0	
21	l-$C_3H_2^+$ + CH_2CCH_2 → c-$C_6H_5^+$ + H	-254	6.0E-11	0	0	[e] Anicich et al. (1984) and new experiment at the SOLEIL synchrotron using the CERISES setup (in preparation)
	c-$C_3H_2CCH^+$ + CH_3	-178	1.2E-10	0	0	
	$CH_2CCCH_2^+$ + C_2H_2	-176	5.8E-10	0	0	
	$C_4H_3^+$ + C_2H_3	-36	4.0E-11	0	0	
	$C_4H_2^+$ + C_2H_4	-108	1.0E-10	0	0	
	c-$C_3H_3^+$ + C_3H_3	-195	3.2E-10	0	0	
22	c-$C_3H_2^+$ + C_3H_6 → c-$C_6H_7^+$ + H	-298	4.5E-10	-0.5	0	[e] Branching ratio from Prodnuk et al. (1992) and new experiment at the SOLEIL synchrotron using the CERISES setup (in preparation)
	c-$C_3H_2CHCH_2^+H^+$ + CH_3	-180	2.5E-10	-0.5	0	
	c-$C_3H_2CH_2^+$ + C_2H_4	-183	1.5E-10	-0.5	0	
	c-$C_3H_3^+$ + C_3H_5	-15	0			
	l-$C_3H_3^+$ + C_3H_5	-155	1.5E-10	-0.5	0	
23	l-$C_3H_2^+$ + C_3H_6 → c-$C_6H_7^+$ + H	-354	4.5E-10	-0.5	0	[e] Branching ratio from Prodnuk et al. (1992) and new experiment at the SOLEIL synchrotron using the CERISES setup (in preparation)
	c-$C_3H_2CHCH_2^+H^+$ + CH_3	-235	2.5E-10	-0.5	0	
	c-$C_3H_2CH_2^+$ + C_2H_4	-238	1.5E-10	-0.5	0	
	c-$C_3H_3^+$ + C_3H_5	-70	7.5E-11	-0.5	0	
	l-$C_3H_3^+$ + C_3H_5	-210	7.5E-11	-0.5	0	
24	l-$C_3H_3^+$ + H_2 → $C_3H_5^+$ + hν	-234	4.0E-18	-3.0	0	See text
25	l-$C_3H_3^+$ + t−C_3H_2 → c-$C_6H_4^+$ + H	-168	1.0E-09	0.0	0	similar rate to l-$C_3H_3^+$ + C_2H_2 and l-$C_3H_3^+$ + C_2H_4 Anicich (2003)
26	l-$C_3H_3^+$ + c−C_3H_2 → c-$C_6H_4^+$ + H	-113	5.0E-10	-0.5	0	similar rate to l-$C_3H_3^+$ + C_2H_2 and l-$C_3H_3^+$ + C_2H_4 Anicich (2003)
	c-$C_3H_2CCCH^+$ + H	-114	5.0E-10	-0.5	0	
27	l-$C_3H_3^+$ + C_3H_3 → c-$C_6H_5^+$ + H	-199	5.0E-10	0	0	[f]
	$CH_2CCHCHCCH^+$ + H	-87	0			
	c-$C_6H_4^+$ + H_2	-144	0			
	c-$C_3H_2CH_2^+$ + C_2H_2	-169	5.0E-10	0	0	
	c-$C_3H_3^+$ + C_3H_3	-140	0			
28	l-$C_3H_3^+$ + CH_3CCH → c-$C_6H_5^+$ + H_2	-245	2.8E-09	-0.5	0	[g]
	c-$C_6H_6^+$ + H	-188	2.1E-10	-0.5	0	
	c-$C_3H_2CH_3^+$ + C_2H_2	-187	4.0E-10	-0.5	0	
	$C_4H_3^+$ + C_2H_4	-56	5.1E-11	-0.5	0	
29	l-$C_3H_3^+$ + CH_2CCH_2 → c-$C_6H_5^+$ + H_2	-245	2.2E-09	0	0	[h]
	c-$C_6H_6^+$ + H	-188	1.2E-10	0	0	
	c-$C_3H_2CH_3^+$ + C_2H_2	-187	1.7E-10	0	0	
	$C_4H_3^+$ + C_2H_4	-56	3.2E-11	0	0	

Table A.1. continued.

#	Reaction	ΔH_R	α	β	γ	ref
30	l-$C_3H_3^+$ + C_3H_6 → c-$C_6H_7^+$ + H_2	-350	1.0E-10	-0.5	0	SOLEIL experiment (to be published). A previous experiment had identified $C_4H_5^+$ as a product Harrison (1963).
	c-$C_6H_5^+$ + H_2 + H_2	-94	1.0E-10	-0.5	0	
	c-$C_5H_6^+$ + CH_3	-118	1.0E-10	-0.5	0	
	c-$C_5H_5^+$ + CH_4	-208	4.0E-11	-0.5	0	
	$C_4H_7^+$ + C_2H_2	-130	2.5E-10	-0.5	0	
	$C_4H_5^+$ + C_2H_4	-120	7.0E-10	-0.5	0	
	$C_2H_5^+$ + $C_2H_3C_2H$	-25	1.0E-09	-0.5	0	
31	l-$C_3H_3^+$ + C_4H_2 → c-$C_3H_3^+$ + C_4H_2	-140	1.1E-09	0	0	Anicich (2003)
	$H_2C_5H^+$ + C_2H_2	-64	3.4E-10	0	0	
32	$C_3H_4^+$ + c-C_3H_2 → c-$C_6H_5^+$ + H	-242	2.0E-10	-0.5	0	[i]
	c-$C_3H_2CH_2^+$ + C_2H_2	-212	1.0E-09	-0.5	0	
	C_3H_3 + c-$C_3H_3^+$	-183	1.0E-10	-0.5	0	
33	$C_3H_4^+$ + C_3H_3 → c-$C_6H_5^+$ + H_2	-331	1.0E-09	0	0	We assume same rate and branching ratio that the isoelectronic l-$C_3H_3^+$ + CH_2CCH_2 reaction.
	c-$C_6H_6^+$ + H	-269	1.0E-10	0	0	
	$C_4H_5^+$ + C_2H_2	-186	1.0E-10	0	0	
34	$C_3H_4^+$ + CH_3CCH → c-$C_6H_7^+$ + H	-213	7.5E-10	-0.5	0	Anicich (2003); Anicich et al. (2003); McEwan & Anicich (2007).
	$C_3H_5^+$ + C_3H_3	+9	3.5E-10	-0.5	0	
35	$C_3H_4^+$ + CH_2CCH_2 → c-$C_6H_7^+$ + H	-213	8.0E-10	0	0	Anicich (2003); Anicich et al. (2003).
	c-$C_6H_6^+$ + H	+9	3.0E-10	0	0	
36	l-$C_3H_5^+$ + H_2 → $C_3H_7^+$ + hν	-234	1.0E-18	-3.0	0	/ l-$C_3H_3^+$ + H_2
37	$C_3H_5^+$ + c-C_3H_2 → c-$C_6H_6^+$ + H	-240	0			[j]
	c-$C_6H_5^+$ + H_2	-302	5.0E-10	-0.5	0	
	c-$C_3H_2CH_3^+$ + C_2H_2	-238	5.0E-10	-0.5	0	
	CH_3CCH + c-$C_3H_3^+$	-191	1.0E-10	-0.5	0	
	CH_2CCH_2 + c-$C_3H_3^+$	-191	1.0E-10	-0.5	0	
38	$C_3H_5^+$ + C_3H_3 → c-$C_6H_7^+$ + H	-221	8.0E-10	0	0	/ $C_3H_4^+$ + CH_3CCH, $C_3H_4^+$ + CH_2CCH_2 Anicich (2003); Anicich et al. (2003); McEwan & Anicich (2007)
39	$C_3H_5^+$ + CH_3CCH → c-$C_6H_7^+$ + H_2	-273	7.0E-10	-0.5	0	Anicich et al. (2006)
40	$C_3H_5^+$ + CH_2CCH_2 → c-$C_6H_7^+$ + H_2	-273	7.0E-10	0	0	/ $C_3H_5^+$ + CH_3CCH
41	$C_4H_2^+$ + C_2H_4 → c-$C_6H_5^+$ + H	-145	7.2E-10	0	0	Anicich et al. (2006).
	c-$C_6H_4^+$ + H_2	-149	7.0E-11	0	0	
	$CH_2CCCH_2^+$ + C_2H_2	-68	7.0E-10	0	0	
42	$C_4H_3^+$ + C_2H_2 → l-$C_6H_5^+$ + hν	-244	2.2E-10	0	0	Anicich (2003); Anicich et al. (2006); Knight et al. (1987); Kocheril et al. (2025); Peverati et al. (2016)
43	$C_4H_3^+$ + C_2H_4 → c-$C_6H_5^+$ + H_2	-189	1.2E-10	0	0	McEwan & Anicich (2007) c-$C_6H_5^+$ is likely the phenylium (see Fig. A.2.5)
44	$C_4H_3^+$ + $C_2H_3C_2H$ → $C_6H_5C_2H^+$ + H	-176	1.1E-10	-0.5	0	Anicich et al. (1984).
	c-$C_6H_5^+$ + C_2H_2	-196	7.2E-10	-0.5	0	
	$C_4H_5^+$ + C_4H_2	-57	1.1E-10	-0.5	0	
45	$C_4H_4^+$ + C_2H_2 → l-$C_6H_5^+$ + H	-89	9.0E-11	0	0	[k] Anicich (2003)
	c-$C_6H_4^+$ + H_2	-92	1.0E-11	0	0	
46	$C_4H_4^+$ + C_2H_4 → l-$C_6H_7^+$ + H	-174	8.0E-10	0	0	[k] Branching ratio deduced using Zyubina et al. (2008).
	c-$C_6H_6^+$ + H_2	-281	2.0E-10	0	0	
47	$C_4H_4^+$ + CH_3CCH → l-$C_7H_7^+$ + H	-284	1.0E-09	-0.5	0	[k] Products from Anicich et al. (1984).
48	$C_4H_4^+$ + $CHCCH_2$ → l-$C_7H_7^+$ + H	-284	1.0E-09	0	0	[k] /$C_4H_4^+$ + CH_3CCH

Table A.1. continued.

#	Reaction	ΔH_R	α	β	γ	ref
49	$C_4H_4^+ + C_4H_2 \rightarrow$ l-$C_6H_5^+ + H$	-86	7.0E-10	0	0	[k] Anicich et al. (1984)
	$C_8H_6^+ + h\nu$	-488	1.0E-10	0	0	
50	$C_4H_5^+ + C_2H_2 \rightarrow$ l-$C_6H_5^+ + H_2$	-145	1.0E-09	0	0	/ $C_4H_3^+ + C_2H_4$
51	$C_4H_5^+ + C_2H_4 \rightarrow$ l-$C_6H_7^+ + H_2$	-230	1.0E-09	0	0	/ $C_3H_5^+ + CH_3CCH$
52	$C_4H_5^+ + CH_3CCH \rightarrow$ c-$C_6H_5^+ + CH_4$	-964	8.0E-10	-0.5	0	Branching ratio from Anicich
	c-$C_7H_7^+ + H_2$	-340	2.0E-10	-0.5	0	et al. (1984).
	$C_6H_5CH_2^+ + H_2$	-310	2.0E-10	-0.5	0	
53	$C_4H_5^+ + C_4H_2 \rightarrow$ l-$C_6H_5^+ + C_2H_2$	-139	1.0E-09	0	0	Branching ratio from Anicich et al. (1984).
54	$C_5H_2^+ + CH_4 \rightarrow$ c-$C_6H_5^+ + H$	There is a barrier equal to +9.8 kJ/mol at M06-2X/AVTZ level for the most stable $C_5H_2^+$ isomer (HC_5H^+)				
55	$C_5H_3^+ + CH_3CCH \rightarrow$ c-$C_6H_5^+ + C_2H_2$	-179	4.9E-10	-0.5	0	[l] Branching ratio from Anicich
	$C_6H_5CCH^+ + H$	-160	1.2E-10	-0.5	0	et al. (1984).
56	$C_5H_3^+ + CH_2CCH_2 \rightarrow C_6H_5^+ + C_2H_2$	-179	4.9E-10	0	0	[l] Same as $C_5H_3^+ + CH_3CCH$.
	$C_6H_5CCH^+ + H$	-160	1.2E-10	0	0	
57	c-$C_6H_4^+ + H \rightarrow$ c-$C_6H_5^+ + h\nu$	-423	2.0E-10	0	0	By comparison with c-$C_6H_6^+ + H$
58	c-$C_6H_4^+ + H_2 \rightarrow$ c-$C_6H_6^+ + h\nu$	There is a a small barrier (+4.5 kJ/mol) at M06-2X/AVTZ for the most stable m-$C_6H_4^+$ isomer.				
59	l-$C_6H_5^+ + H \rightarrow$ c-$C_6H_6^+ + h\nu$/c-$C_6H_5^+ + H$	Low rate constant Petrie et al. (1992)				
60	c-$C_6H_5^+ + H_2 \rightarrow$ c-$C_6H_7^+ + h\nu$	-261	6.0E-11	0	0	Ausloos et al. (1989); Keheyan (2001); McEwan et al. (1999); Petrie et al. (1992); Scott et al. (1997); Snow et al. (1998)
61	c-$C_6H_5^+ + CH_4 \rightarrow$ c-$C_7H_7^+ + H_2$	-176	5.0E-11	0	0	Ausloos et al. (1989); Anicich
	$C_6H_5CH_2^+ + H_2$	-145	0			et al. (2006)
62	c-$C_6H_5^+ + C_2H_2 \rightarrow C_6H_5CCH_2^+ + h\nu$	-341	3.0E-10	0	0	Anicich et al. (2003); Knight
	$C_6H_5CCH^+ + H_2$	+20	0			et al. (1987); Loison et al. (2025)
63	c-$C_6H_5^+ + O \rightarrow$ c-$C_5H_5^+ + CO$	-407	6.0E-11	0	0	Scott et al. (2000)
	c-$C_3H_3^+ + H_2C_3O$	-200	4.0E-11	0	0	
64	c-$C_6H_6^+ + H \rightarrow$ c-$C_6H_7^+ + h\nu$	-318	2.2E-10	0	0	Betts et al. (2006); McEwan
	c-$C_6H_5^+ + H_2$	-57	0			et al. (1999); Petrie et al. (1992); Snow et al. (1998) Some $C_6H_5^+$ is produced Betts et al. (2006); McEwan et al. (1999) but will quickly react with H_2 leading to c-$C_6H_7^+$ in ISM.
65	c-$C_6H_6^+ + N \rightarrow$ c-$C_5H_5^+ + HCN$	-229	1.4E-10	0	0	McEwan et al. (1999)
66	c-$C_6H_6^+ + O \rightarrow$ c-$C_5H_6^+ + CO$	-376	9.5E-11	0	0	Scott et al. (1997); Snow et al.
	c-$C_6H_5^+ + H_2$		1.0E-11	0	0	(1998)
67	c-$C_6H_7^+ + O \rightarrow$ c-$C_5H_7^+ + CO$	There is a barrier on the triplet entrance channel at M06-2X/AVTZ level.				
68	$H +$ c-$C_6H_4 \rightarrow$ c-$C_6H_5 + h\nu$	No barrier for Madden et al. (1997) and Castiñeira Reis et al. (2024) but a small barrier (4 kJ/mol) at M06-2X/AVTZ level and a barrier equal to 14 kJ/mol at G96LYP/6-31+G(d,p) level Tseng et al. (2004).				
69	$H +$ c-$C_6H_5 \rightarrow$ c-$C_6H_6 + h\nu$	-458	2.0E-10	0	0	Ackermann et al. (1990); Vuitton et al. (2012)

Table A.1. continued.

#	Reaction	ΔH_R	α	β	γ	ref
70	$H + C_6H_5CH_2 \rightarrow C_6H_5CH_3 + h\nu$	-371	2.0E-10	0	0	Ackermann et al. (1990); Baulch et al. (1994)
71	$C + c\text{-}C_5H_5 \rightarrow c\text{-}C_6H_4 + H$	-293	4.0E-10	0	0	/ $C + c\text{-}C_5H_6$,$C + c\text{-}C_6H_6$
72	$C + c\text{-}C_5H_6 \rightarrow c\text{-}C_6H_5 + H$	-311	4.0E-10	0	0	/ $C + C_6H_6$, the published experimental value (1.9e-9 $cm^3\ s^{-1}$) Haider & Husain (1993a) seems overestimated for a neutral-neutral reaction.
73	$C + c\text{-}C_6H_4 \rightarrow t\text{-}C_3H_2 + C_4H_2$	-205	4.0E-10	0	0	/ $C + c\text{-}C_6H_6$.
74	$C + c\text{-}C_6H_6 \rightarrow c\text{-}C_5H_4CCH + H$ $CH_3C_4H + C_2H_2$	-103 -164	4.0E-10 0	0	0	[m] Bergeat & Loison (2001); Haider & Husain (1993b); Hahndorf et al. (2002); Kaiser et al. (1999); da Silva (2014)
75	$C + C_6H_5C_2H \rightarrow c\text{-}C_9H_5 + H$	-31	4.0E-10	0	0	/ $C + c\text{-}C_6H_6$.
76	$C + C_6H_5CN \rightarrow C_6H_4C_2N + H$	-74	4.0E-10	0	0	/ $C + c\text{-}C_6H_6$.
77	$CH + CH_3C_4HN \rightarrow l\text{-}C_6H_4 + H$	-310	4.0E-10	0	0	Very likely without a barrier, but producing likely linear isomer Castiñeira Reis et al. (2024).
78	$CH + H_2C_3HC_2H \rightarrow l\text{-}C_6H_4 + H$	-355	4.0E-10	0	0	Very likely without barrier but producing likely linear isomer.Castiñeira Reis et al. (2024).
79	$CH + c\text{-}C_5H_6 \rightarrow c\text{-}C_6H_6 + H$	-439	4.0E-10	0	0	Products from Caster et al. (2021).
80	$CH + c\text{-}C_6H_6 \rightarrow c\text{-}C_7H_6 + H$	-54	4.0E-10	0	0	/ Rate from Berman et al. (1982).
81	$CH_2 + c\text{-}C_5H_5 \rightarrow c\text{-}C_6H_6 + H$	-346	1.0E-10	0	0	minor reaction.
82	$CH_3 + HC_5H \rightarrow l\text{-}C_6H_4 + H$	-163	1.0E-10	0	0	Very likely without barrier but benzyne production needs several isomerization Castiñeira Reis et al. (2024).
83	$CH_3 + H_2C_5 \rightarrow l\text{-}C_6H_4 + H$	-156	1.0E-10	0	0	Very likely without barrier but benzyne production needs several isomerization Castiñeira Reis et al. (2024).
84	$C_2 + CH_2CHCHCH_2 \rightarrow c\text{-}C_6H_5 + H$	Very likely without barrier but complex pathway Castiñeira Reis et al. (2024).				
85	$C_2H + C_2H_3C_2H \rightarrow l\text{-}C_6H_4 + H$ $c\text{-}C_6H_4 + H$	-131 -167	1.8E-10 2.0E-11	0 0	0 0	Zhang et al. (2011) with a rate similar to $C_2H + C_4H_2$ Landera et al. (2008) and $C_2H + C_4H_6$ Jones et al. (2011)
86	$C_2H + CH_2CHCHCH_2 \rightarrow c\text{-}C_6H_6 + H$ $l\text{-}C_6H_6 + H$	-384 -122	1.0E-10 1.0E-10	0 0	0 0	Jones et al. (2011); Lee et al. (2019)
87	$C_2H + c\text{-}C_6H_6 \rightarrow C_6H_5C_2H + H$	-114	3.28E-10	-0.18	0	Goulay & Leone (2006); Woon (2006).
88	$C_2H_3 + C_4H_3 \rightarrow c\text{-}C_6H_5 + H$	-235	4.0E-11	0	0	Duran et al. (1988) and Castiñeira Reis et al. (2024), linear $l\text{-}C_6H_5$ isomers may also be produced.
89	$C_3 + C_3H_5 \rightarrow c\text{-}C_6H_4 + H$ $C_2H_3C_4H + H$ $HCCCHCHCCH + H$	-313 -277 -265	5.0E-11 5.0E-12 5.0E-12	0 0 0	0 0 0	[n]

Table A.1. continued.

#	Reaction	ΔH_R	α	β	γ	ref
90	l-C_3H_2 + C_3H_3 → $H_2C_6H_2$ + H	-133	5.0E-11	0	0	[o]
	$CH_2CCCHCCH_2$	-363	0			
	c-C_6H_4 + H	-216	0			
91	C_3H_3 + C_3H_3 → c-C_6H_5 + H	-149	1.0E-10	0	0	[p]
	c-C_6H_6 + hν	-607	0			
92	C_4H + C_2H_4 → $C_2H_3C_4H$ + H	-122	3.0E-10	0	0	[q]
	c-C_6H_4 + H	-158	0			
93	CN + c-C_6H_6 → C_6H_5CN + H	-100	4.0E-10	0	0	Trevitt et al. (2009).
94	O + c-C_6H_5 → c-C_5H_5 + CO	-420	1.1E-10	0	0	Frank et al. (1994).
95	O + c-C_7H_5 → c-C_6H_5 + CO	-539	1.0E-10	0	0	Trevitt et al. (2009).
96	c-$C_6H_4^+$ + e^- → l-C_6H_2 + H + H	-239	1.0E-06	-0.3	0	/ $C_6H_6^+$ + e^-
	C_4H_2 + C_2H_2	-652	1.0E-06	-0.3	0	
97	l-$C_6H_5^+$ + e^- → c-C_6H_4 + H	-441	1.2E-06	-0.3	0	Fournier et al. (2013)
98	c-$C_6H_5^+$ + e^- → $C_2H_3C_4H$ + H	-511	1.0E-06	-0.3	0	[r]
	c-C_6H_4 + H	-547	1.0E-06	-0.3	0	
	l-C_6H_2 + H + H_2	-349	0			
99	c-$C_6H_6^+$ + e^- → c-C_6H_5 + H	-432	1.1E-06	-0.69	0	[s]
	c-C_6H_4 + H_2	-503	1.0E-07	-0.69	0	
	C_3H_3 + C_3H_3	-283	1.0E-07	-0.69	0	
100	c-$C_6H_7^+$ + e^- → c-C_6H_6 + H	-572	1.8E-06	-0.83	0	[t]
	c-C_6H_4 + H + H_2	-185	1.0E-07	-0.83	0	
	c-C_6H_5 + H + H	-113	1.0E-07	-0.83	0	
101	$C_6H_5CCH_2^+$ + e^- → $C_6H_5C_2H$ + H	-482	2.0E-06	-0.83	0	[u]
102	$C_6H_5CNH^+$ + e^- → C_6H_5CN + H	-500	1.5E-06	-0.83	0	[v]
	c-C_6H_5 + HCN	-465	2.5E-07	-0.83	0	
	c-C_6H_5 + HNC	-413	2.5E-07	-0.83	0	

[a] Rate constant using capture rate theory Georgievskii & Klippenstein (2005). Using the calculations of Peverati et al Peverati et al. (2016) for the $C_4H_3^+$ + C_2H_2 reaction, and considering the exothermicity notably higher than for the $C_4H_3^+$ + C_2H_2 reaction, we assume that the isomerization toward the cyclic isomer is favored. The exothermicity is given for l-C_6H_4 = $C_2H_3C_4H$.

[b] Rate constant using capture rate theory Georgievskii & Klippenstein (2005). l-C_6H_6($CH_2CHCHCHCCH$) is supposed to be produced in the C_2H + $CH_2CHCHCH_2$ reaction Jones et al. (2011). The TSs from l-$C_6H_7^+$ to $C_6H_7^+$ are located much below the exothermicity of the reaction as can be seen in Fig. A.2.1. As noted by Herbst et al Herbst et al. (2000), the typical time-scales for isomeric conversion is much shorter than for relaxation by one infrared photon emission. Thus, as relaxation occurs slowly, isomeric conversion leads to equilibrated isomeric abundances at each internal energy. The final balance is determined at or near the effective barriers to isomerization, which corresponds to the energy of the transition states favoring $C_6H_7^+$. Some $C_6H_7^+$ may dissociate into $C_6H_7^+$ + H_2.

[c] Considering M06-2X/AVTZ calculations shown in Fig. A.2.2 with cyclization in few steps with fairly low TS, and by comparison with the isoelectronic l-$C_3H_3^+$ + C_3H_4 reaction, the formation of $C_6H_5^+$ should be significant.

[d] The first step is $CH_2CH_2CHCCCH^+$ formation which self-isomerize into c-$C_3H_5CCCH^+$. The TS from c-$C_3H_5CCCH^+$ → c-$C_4H_5CCH^+$ is located -187 kJ/mol below the entrance channel as shown in Fig. A.2.3. We use similar branching ratio than for $C_4H_2^+$ + C_2H_4 Anicich et al. (2006) (with the fact that the more energy is put into the system, the more $C_6H_5^+$ is disadvantaged when compared to $C_3H_2^+$ + C_3H_4 using Anicich et al. 1984).

[e] There are three isomers for $C_3H_2^+$: c-$C_3H_2^+$ (the most stable), $HCCCH^+$ (+55 kJ/mol called l-$C_3H_2^+$ but is in fact the t-$C_3H_2^+$ using the nomenclature of the neutral) and H_2CCC^+ (+196 kJ/mol not present in the network and is in fact the real l-$C_3H_2^+$ using the nomenclature of the neutral). Experimentally, both c-$C_3H_2^+$ and HCCCH+ isomers are produced and are not separated. They generally have similar reactivity, except with water Prodnuk et al. (1992), and we consider the same rate constants and branching ratios for both isomers.

[f] Considering the M06-2X/AVTZ calculations shown in Fig. A.2.4 with cyclization in few steps with fairly low TS, we use similar branching ratio than for $C_4H_2^+$ + C_2H_4 Anicich et al. (2006) (with the fact that the more energy is put into the system, the more $C_6H_5^+$ is disadvantaged when compared to $C_3H_2^+$ + C_3H_4 using Anicich et al. (1984)).

[g] We performed new experiments at SOLEIL synchrotron using the CERISES setup (to be published) showing that l-$C_3H_3^+$ is reactive with CH_3CCH as it is reactive with C_2H_2, C_2H_4, C_4H_2 ... Anicich (2003). In Anicich et al. (1984) they cited old branching ratios : $C_6H_5^+$ + H_2 (45%), $C_4H_5^+$ + C_2H_2 (35%) and $C_4H_3^+$ + C_2H_4 (20%).

[h] We performed new experiments at SOLEIL synchrotron using the CERISES setup (to be published) showing that l-$C_3H_3^+$ is reactive with CH_2CCH_2 as it is reactive with C_2H_2, C_2H_4, C_4H_2 ... Anicich (2003). In Anicich et al. (1984) they cited old branching ratios : $C_6H_5^+$ + H_2 (38%), $C_4H_5^+$ + C_2H_2 (37%) and $C_4H_3^+$ + C_2H_4 (25%).

[i] There is probably no barrier compared to the reactions of $C_3H_4^+$ with C_2H_2 and C_2H_4. We consider similar rate and branching ratio than for the $C_4H_2^+ + C_2H_4$ reaction Anicich et al. (2006) (with the fact that the more energy is put into the system, the more $C_6H_5^+$ is disadvantaged when compared to $C_3H_2^+ + C_3H_4$ using Anicich et al. (1984)). Moreover, the production of c-$C_3H_2CH_2^+$ requires few steps and is likely favoured.

[j] There is probably no barrier compared to the reactions of $C_3H_5^+$ with C_2H_2 and C_2H_4. Since the hydrogen atoms are distributed across all the carbons, cyclization into $C_6H_7^+$ requires few steps and is probably favored. We assume similar rate and branching ratio that the isoelectronic l-$C_3H_3^+ + CH_2CCH_2$ reaction favoring the c-$C_3H_2CH_3^+$ production.

[k] the most stable isomer for $C_4H_4^+$ is c-$C_3H_2CH_2^+$ (then $CH_2CCCH_2^+$: +47 kJ/mol, CH_2CHCCH^+: +58 kJ/mol (used for the exothermicities of the reactions), c-$C_4H_4^+$: +59 kJ/mol). The various $C_4H_4^+$ isomers have not the same reactivity

[l] The most stable isomer for $C_5H_3^+$ is c-$C_3H_2CCH^+$ rather than $H_2C_5H^+$ (+83 kJ/mol). We have little information about the nature of the isomers studied in the few experiments that have been conducted but $C_5H_3^+$, produced from l-$C_3H_3^+ + C_4H_2$, is reactive with C_4H_2 Ozturk et al. (1989). In astrochemical models, there are several effective sources of $C_5H_3^+$: c,t,l-$C_5H_2 + H_3^+/HCO^+$, c,l-$C_3H_2^+ + C_2H_2$, $CH_3C_4H + He^+$ .... Both c-C_3H_2CCH andH_2C_5H are likely to be produced.

[m] The exit channels on the triplet surface are not very exothermic which should favor intersystem crossing toward the singlet surface. The rate constant has been measured at room temperature and low pressure. C_7H_5 has been clearly identified in crossed molecular beam experiment without branching ratio determination Hahndorf et al. (2002); Kaiser et al. (1999). The most favorable bimolecular products seems to be c-C_5H_4CCH + H according to da Silva (2014).

[n] There is no barrier at level M06-2X/AVTZ (Fig. A.1.1) for the addition of C_3 to C_3H_5(CH_2CHCH_2 most stable isomer Stranges et al. (2008)), yielding the adduct CH_2CHCH_2CCC (similar to the absence of barrier for the C_3 to C_3H_3 reaction Mebel et al. (2023)). This adduct can evolve either by direct loss of hydrogen to yield a linear isomer of C_6H_4 or, more favorably, to yield C_6H_4 (cyclic) + H (Fig. A.1.2). The rates proposed are approximate and will require further calculations (and experiments).

[o] No barrier in the entrance valley according to Castiñeira Reis et al. (2024) leading to $CH_2CCCHCCH_2$ and CH_2CCCH_2CCH. The pathway from $CH_2CCCHCCH_2$ to C_6H_5 involve various TS as high as -93 kJ/mol below the l-$C_3H_2 + C_3H_3$ entrance level Castiñeira Reis et al. (2024), so some C_6H_4 may be produced.

[p] Georgievskii et al. (2007); Miller & Klippenstein (2003); Vuitton et al. (2019); Hrodmarsson et al. (2024). We neglect the C_6H_6 formation (various isomers) at very low pressure.

[q] Rate derived from Berteloite et al. (2010), the experimental values being valid in the 39-300K range. The isomerization toward benzyne likely involve high TS using Castiñeira Reis et al. (2024) (even if $CH_2CH_2C_4H$ isomer was not considered in Castiñeira Reis et al. (2024)).

[r] The pathway for $C_2H_3C_4H \rightarrow C_6H_4$ involves 3 TS located as high as 367 kJ/mol above the $C_2H_3C_4H$ energy Castiñeira Reis et al. (2024). Moreover, he pathway for the various C_6H_5 isomers toward the cyclic one involve TS as low as 370 kJ/mol above the l-C_6H_5 energy so isomerization of C_6H_5 before C-H dissociation is possible.

[s] Rate constant from Hamberg et al. (2011), branching ratio guessed by comparison with C_6H_6 photodissociation.

[t] Global rate from Hamberg et al. (2011) with the preserved cycle.

[u] Same rate as $C_6H_6^+ + e^-$. Large uncertainties, $C_6H_6 + C_2H$ and $C_6H_6 + C_2H_2$ may also be produced.

[v] Same rate as $C_6H_6^+ + e^-$.

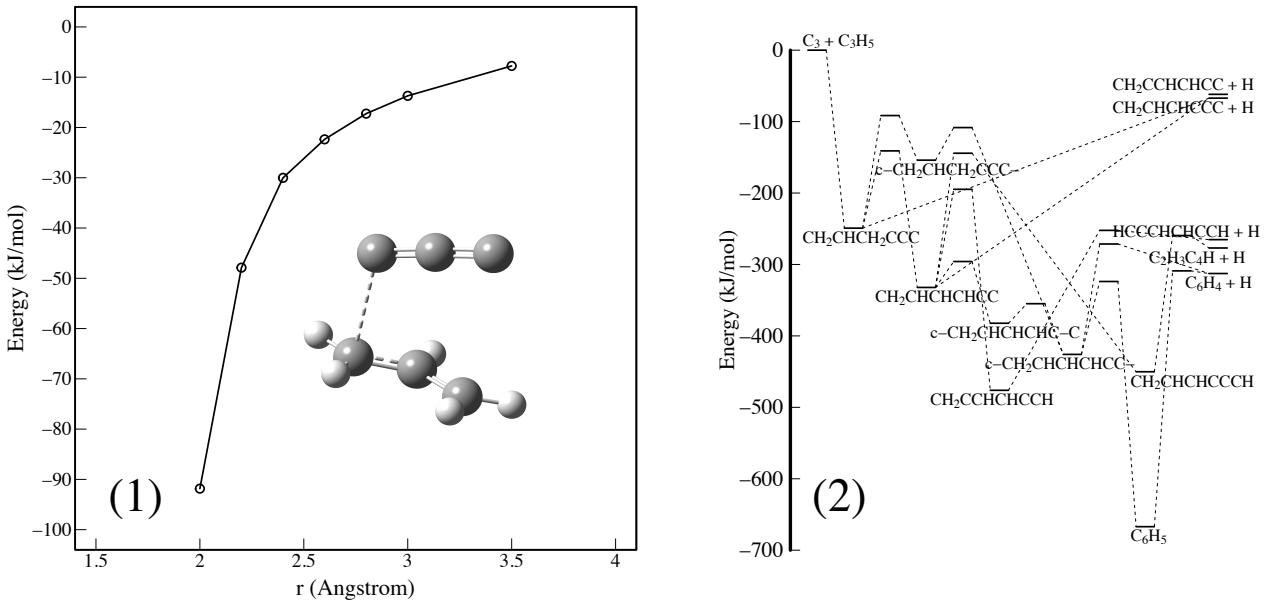

Fig. A.1. Relaxed energy approach (panel 1) and simplified diagram of potential energy (panel 2) for $C_3 + C_3H_5$ reaction calculated at the M06-2X/AVTZ level.

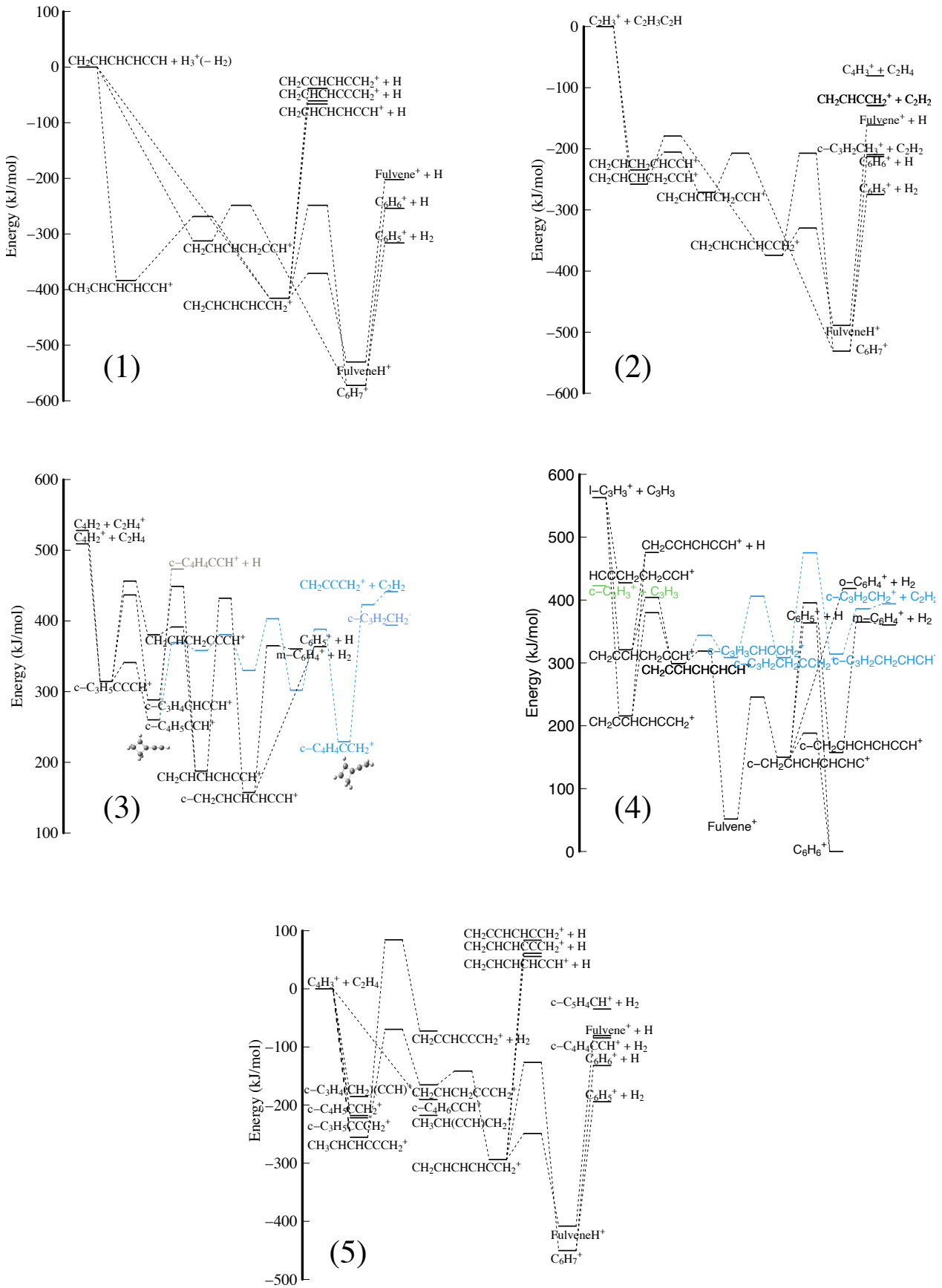

Fig. A.2. Simplified diagrams of potential energy for H_3^+ + l-C_6H_6($H_2CHCHCHCCH$) (panel 1), $C_2H_3^+$ + $C_2H_3C_2H$ (panel 2), $C_2H_4^+$ + C_4H_2 and C_2H_4 + $C_4H_2^+$ (panel 3), $C_3H_3^+$ + C_3H_3 (panel 4), and $C_4H_3^+$ + C_2H_4 (panel 5) reactions, calculated at the M06-2X/AVTZ level.